Seven-Element Ground Skirt Monopole ESPAR Antenna Design From a Genetic Algorithm and the Finite Element Method

Seven-Element Ground Skirt Monopole ESPAR Antenna Design From a Genetic Algorithm and the Finite Element Method

Robert Schlub, Junwei Lu, *Member, IEEE*, and Takashi Ohira, *Senior Member, IEEE*

***Abstract*—The design of an optimized Electronically Steerable Passive Array Radiator (ESPAR) antenna is presented. A genetic algorithm using a finite element based cost function optimized the antenna's structure and loading conditions for maximal main lobe gain in a single azimuth direction. Simulated gain results of 7.3 dBi at 2.4 GHz were attained along the antenna's elemental axis. The optimized antenna was fabricated and tested with the corresponding experimental gain better than 8 dBi. The 0.7 dB error between simulated and measured gain was constant for numerous structures and therefore did not affect the optimization. The optimized antenna reduced average main lobe elevation by 15.3° to just 9.7° above the horizontal.**

***Index Terms*—Antennas, genetic algorithm, parasitic radiator, smart antennas.**

I. Introduction

SMART antenna technology will play a crucial role in future wireless communication networks and systems. Present-day networks, be they mobile communication or local computer networks, are struggling under increasing user demand and limited, expensive spectrum. Common techniques to increase system gain and user density capabilities such as TDMA, CDMA, cell splitting, etc. are rapidly approaching their limitations. However, their effectiveness can be extended by combining them with space division multiple access (SDMA) [1]. To utilize SDMA in a wireless system, antennas that can discriminate signals spatially are required. A host of electrically beam steerable adaptive antenna arrays have existed for some time. Typically, each element is excited with different phases of the information signal to form radiation beams and nulls. However, inherent complexity has restricted the use of conventional adaptive arrays in massively produced communication products, like user terminals. To address this, electrically steerable or switchable parasitic antenna arrays have been introduced [2]–[6].

The Electronically Steerable Passive Array Radiator (ESPAR) is one such antenna that is being developed for use in wireless *ad hoc* computer networks [4]–[6]. Wireless *ad hoc* networks are autonomous to infrastructure like base-stations and cabling. This makes them a cheap and simple solution compared to existing wired networks. However, wireless systems are susceptible to signal errors arising from multipath propagation and interference signals from unsolicited nodes. As data is multihopped, signal errors between just a few intermediate nodes can have a potentially devastating effect on the entire network performance. In addition, wireless transmission can be a significant drain on the node's stored energy. Node battery life is shortened considerably if high transmission powers are required for efficient communication.

The ESPAR antenna can direct radiation at intended recipients and steer radiation nulls toward the interfering signals. As a result, such problems are significantly reduced. The radiation nulls and main lobe gains complement each other to maximize the system signal to interference noise ratio. Furthermore, the antenna's main lobe gain dramatically decreases the required transmission power for a set range. Directed radiation also helps alleviate health concerns that might accompany such a device.

The antenna consists of a single feed element surrounded by a ring of reactively loaded parasitic elements. By electrically controlling the loading reactances, directional beams and nulls can be formed and steered throughout the azimuth. Thus the physical structure of the antenna is simple and requires relatively little power to operate when compared to its phased array counterparts.

However, the strong electromagnetic coupling between elements and finite ground structure make the antenna's analytical solution very complex. Accordingly, computational modeling is required to determine the antenna characteristics without experimental testing. Due to this complexity, relatively little effort has been made to determine the optimum structure of the antenna for best performance.

To address this, a genetic algorithm (GA) was employed in conjunction with an FEM based cost function in order to optimize the antenna structure. The GA's stochastic nature ensures a robust process that is less likely to be trapped in localized minima compared to its deterministic counterparts [7]. This is an essential trait as the ESPAR antenna has many optimizable variables and, hence, a large solution space. FEM was used as the cost function of the GA in order to obtain highly accurate solutions. If an inaccurate cost function were used, the optimization error would be pronounced because the ESPAR antenna's electrical performance is very sensitive to its physical dimensions. In addition, FEM's nonuniform meshing allowed accurate yet efficient modeling of the structure.

Manuscript received April 28, 2002; revised November 12, 2002. This work was supported in part by the Telecommunications Advancement Organization of Japan under Grant.

R. Schlub and J. Lu are with the Radio Science Laboratory, School of Microelectronic Engineering, Griffith University, Nathan, QLD 4111 Australia (e-mail: r.schlub@griffith.edu.au; J.Lu@griffith.edu.au).

T. Ohira is with the ATR Adaptive Communications Research Laboratories, Kyoto 619-0288, Japan (e-mail: ohira@atr.co.jp).

Digital Object Identifier 10.1109/TAP.2003.818790

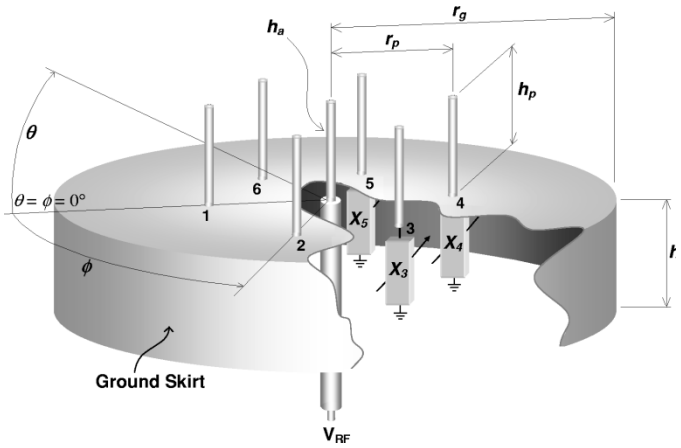

Fig. 1. ESPAR antenna structure.

The genetic optimization focused on improving the main-lobe horizontal gain of the antenna. In doing so, both radiation sensitivity at side angles and transmitter power are reduced. This is even more pronounced in an *ad hoc* network where nodes utilize the same antenna type. In the majority of signal environments, it is conceivable that the transmitting and receiving antennas will be operating with positive gain in their propagation direction. The gains from both antennas will combine to define system performance. As a result, any design improvement made in the antenna's gain will potentially have double the effect in a system.

First, the initial structure and basic ESPAR operating principles will be introduced followed by the procedure used to optimize the gain of the antenna. The results of the optimization will be shown with simulations verified through experimental procedure. For complete specifications and protocols of the *ad hoc* network the antenna is to be implemented in see [8].

II. ESPAR Antenna Configuration

Similar to conventional adaptive arrays, the ESPAR antenna is an adaptive solution that can create and steer both radiation lobes and nulls in arbitrary directions. In contrast however, the ESPAR antenna's beam forming elements are all passive in nature and do not require complex feeding networks and control systems. Typically, the parasitic elements are base-loaded with varactor diodes whose voltage controlled reactances produce different antenna radiation patterns. The dc controlled varactors allow simple electrically formed radiation with minimal power expense. Its uncomplicated structure and low-power operation make the antenna an ideal candidate for massively produced user terminals.

A seven element antenna (Fig. 1) is considered where a single feed monopole is encircled by six, equally spaced, parasitic monopole elements. The antenna elements reside on a hollowed cylindrical ground structure, under which the parasitic elements are loaded. While this ground configuration consumes substantially more volume than would be required for the complementary dipole array, it provides a practical, mechanically sound solution for antenna feeding and control circuitry. Table I defines the antenna dimensions including active monopole height h_a, parasitic monopole height h_p, skirt height h_s, parasitic radius r_p, and ground radius r_g. Initially, the antenna was designed for

TABLE I
INITIAL STRUCTURE OF THE ESPAR ANTENNA

Length	Structural Dimensions				
	r_g	r_p	h_a	h_p	h_s
mm	60	30	28	28	30
λ (2.4GHz)	0.48	0.24	0.224	0.224	0.24

2.484 GHz, but experimental resonance was found at 2.4 GHz. Therefore, the antenna optimization, and hence its definition in Table I, is also at 2.4 GHz.

The ground skirting is used to reduce the radiation lobe elevation that exists due to the finite ground plane dimensions [9], [10]. Indoors, ceilings often provide unobstructed reflections, thus reducing the main-lobe elevation not only increases the azimuth gain, but also reduces the likelihood of multipath interference.

The original structure in Table I was designed using fundamental design techniques in conjunction with heuristic experience and therefore, it was not known whether all dimensions were optimal. While the structure is relatively simple, the electrical analysis of the antenna is complex, and hard to optimize analytically. Therefore, the finite element based commercial software package High Frequency Structure Simulator (HFSS) [11] was used together with a GA to simulate and optimize the structure.

The antenna itself raises a host of questions regarding its functionality. Answers to these questions are under different stages of investigation, but preliminary results have been published. These include the required beam-forming algorithm [12], [13], the radiation beam sensitivity with respect to reactance [14] and the diode nonlinearity under typical transmission powers [15].

III. Optimization Procedure

The gain of the antenna is a defining feature in the performance of an *ad hoc* wireless network. Thus, the optimization goal was simply to maximize directional gain in a single azimuth direction. Antenna gain is defined as the product of its directivity D and efficiency e [16].

$$G = eD. \tag{1}$$

Conductor ohmic losses are considered negligible, thus only the antenna's impedance mismatch is considered in the efficiency. Equation (1) can then be rewritten

$$G = \left(1 - |S_{11}|^2\right) D \tag{2}$$

which shows optimizing the gain simultaneously optimizes the return loss (S_{11}) and the antenna directivity.

Considering the ESPAR configuration, there are two main areas requiring optimization; the structural dimensions and the reactive loads. However, both the structure and loading reactances couple to determine the radiation characteristics of the antenna, and as such an optimum set of reactance values is unique to a single structure only. Therefore, it was desirable to optimize both reactance values and structure. As this presented a very large solution space, the optimization was partitioned into several consecutive stages that alternated optimization of

reactive loads and structure. Each successive stage's optimization variables underwent an increase in resolution with a decrease in range.

A. Reactance Optimization

With an expensive cost function, the optimization process needs to be as efficient as possible. Referring to Fig. 1, there are six different reactance values that require attention. However, because the optimization goal is to maximize gain in a single azimuth direction, the problem can be simplified by selecting either $\phi = 0°$ or $\phi = 30°$ as the direction of gain optimization. Reactance symmetry around this angular axis can then be used. The two axes reduce the required optimization variables to 4 and 3, respectively. While the $\phi = 0°$ case contains an additional variable, it was assumed that a higher gain would be seen along the elemental axis and was thereby chosen.

The second technique to depress the optimization time was to make the reactance resolution (reactance step between possible values) nonlinear. At the base of the parasitic monopoles are transmission lines connected to loads ($Z_L = R_L + \mathrm{j}X_L$) shorted to ground (see Fig. 3). Therefore, the signal induced in the parasitic element is guided down the transmission line and reflected with some phase shift. The total phase shift (as seen at the monopole base) depends on the reactive load Z_L, the transmission line's (TL) characteristic impedance (Z_O) and the TL's length. Elementary TL theory states that the reflection coefficient (Γ) of a loaded transmission line is [17]

$$\Gamma = \Gamma_r + j\Gamma_i = \frac{Z_L - Z_O}{Z_L + Z_O} \tag{3}$$

where subscripts r and i designate the real and imaginary components of the reflection coefficient. Normalizing with respect to Z_O and assuming no loss in the TL or load ($R_L = 0 \rightarrow |\Gamma| = 1$), (3) can be rearranged to find the angular component of the reflection (Γ_ϕ.).

$$\Gamma_\phi = \arctan\left(\frac{\Gamma_i}{\Gamma_r}\right) = \arctan\left(\frac{2x_L}{x_L^2 - 1}\right). \tag{4}$$

Here, x_L is the load reactance normalized to the TL characteristic impedance. This relationship is well known and best visualized on a Smith Chart. When $|x_L|$ becomes large, there is little change in Γ_ϕ and, hence, there will be insignificant change in the antenna radiation characteristics. Conversely, when $|x_L|$ is near 0, the change in Γ_ϕ with respect to $|x_L|$ is significant. Clearly, a fine, linear reactance resolution for large $|x_L|$ will become an unnecessary burden on the optimizer. As changes in the radiation characteristics with respect to Γ_ϕ would be more pronounced, it was decided to step linearly with respect to Γ_ϕ. The final reactances (X_L) were calculated from rearranging (4)

$$X_L = \frac{\sin(\Gamma_\phi)}{1 - \cos(\Gamma_\phi)} Z_O. \tag{5}$$

As Γ_ϕ is naturally bounded between 0 and 2π, a small, finite set of reactances can be chosen which represent all possible reactance values that would significantly change the characteristics of the antenna. During the initial optimization stage, each reactance was discretized into 64 levels (5 bits) separated by 5.6° in Γ_ϕ. In the later stages of optimization, Γ_ϕ stepping was reduced to less than 1°.

B. Structural Optimization

To reduce optimization time, a limited set of antenna dimensions were optimized (Table I). Monopole radius (1 mm) and skirt sheet thickness (0 mm—a 2-D sheet) were kept constant. It was thought the time cost involved to include these dimensions in the optimization, would outweigh the marginal performance increase they would net.

In contrast to the reactive optimization, the optimization of structural dimensions had to be performed over a restricted range of values. A maximum of 0.2λ variation from the initial dimensions was chosen as the optimization range for the dimensions h_s, r_p, and r_g. Initially, the monopole heights h_a and h_p were close to their theoretical resonance of 0.25λ and therefore were only varied by 0.06λ (7.5 mm) during optimization.

The antenna's electrical characteristics were not uniformly sensitive to all structural dimensions. For instance, variation in h_a or h_p would produce greater changes than the same variation in r_g. Consequently, the optimization resolutions were set empirically for each dimension. During the initial optimization stages, the resolution of r_g was 2 mm, r_p and h_s were stepped by 1.5 mm and the element heights h_a and h_p were resolved to 1 mm. The resolutions of h_a and h_p were refined to 0.5 mm when the optimization was in its final stages.

C. Genetic Algorithm

The purpose of computer optimization is to obtain an automated process that can design an antenna based on predetermined criteria. The problem at hand presented a large solution space and diverse range of optimizable variables. As such, the solution space was likely to contain many near-optimal solutions and be polluted with even more localized suboptimal solutions. Evidently, an optimization algorithm that was unlikely to get trapped in the suboptimal solutions and could converge on different near-optimal solutions simultaneously was required. The GA technique was the obvious choice. It solves globally and is robust to suboptimal solutions due to its inherent stochastic nature [7]. Recently, GAs have successfully been employed to tackle a range of wire and loaded wire antennas for precisely these stated reasons [18]–[20]. A GA can take many different forms depending on the type of coding and selection schemes that are employed. While the schemes that were used with this work will be discussed, the actual mathematical process of the GA will not be shown as there is ample literature already detailing the method [7], [21].

One defining feature of a GA is how the optimization variables are coded into a gene. In this case, direct binary coding was employed. As discussed in Sections III-A and III-B, the optimization variables were discretized over practical limits. Each possible value was then given some index that could be directly coded into the chromosome. The major drawback of using direct binary coding was the discretization, or number of possible gene values, was limited to an integer power of 2.

The mating and replacement selection process implemented was Multiniche crowding (MNC) [22]. This allowed the simultaneous optimization of localized minima through selection based on the similarity of two chromosomes.

TABLE II
OPTIMIZED REACTANCES (jΩ)

X_1	X_2	X_3	X_4	X_5	X_6
-14	-65	39	17	39	-65

TABLE III
OPTIMIZED ESPAR ANTENNA DIMENSIONS

Length	Structural Dimensions				
	r_g	r_p	h_a	h_p	h_s
mm	60	38.5	27	27	34.5
λ (2.4GHz)	0.480	0.308	0.216	0.216	0.276

The GA optimizes a population through analysis of a cost function (fitness function) C. As gain was being optimized, then the cost function was simply from (2)

$$C = \left(1 - |S_{11}|^2\right) D. \tag{6}$$

As the maximum achievable gain of the antenna was unknown, the stopping criterion of the optimizer was simply a generation limit. The generation limit was set at 20, but rarely did the optimization progress this far as the population would become homogeneous.

One of the GA's drawbacks is the fact it requires a large number of cost function calculations. As the maturing population homogenizes, the prospect of encountering a previously solved chromosome increases. Because the finite element cost function calculation time varied between 13 and 20 min, there was risk the optimization time would become unmanageably large. To minimize this, a database of unique antenna configurations (chromosomes) was maintained and referenced during optimization. The fraction of a second required for the optimizer to crosscheck the database with the chromosome under test, was insignificant compared to resimulating the chromosome's corresponding antenna structure.

IV. OPTIMIZATION RESULTS

Employing a dual PIII 850 with 1 GB RAM, the total optimization involving 3799 unique cost function computations took close to four weeks. However, with incessant increases in desktop computer speed, such optimization times will reduce rapidly. Contemporary processors boast clock speeds three times that of the ones used for the presented optimization, and as such, the potential for applying the aforementioned design procedure to similar problems is strong.

Tables II and III show the optimized reactances and antenna dimensions at 2.4 GHz. Comparing the optimized dimensions to Table I, the most significant change is the parasitic radius r_p, which increased by 9.5 mm to almost a third of a wavelength. The ground skirt height was limited to a maximum of 34.5 mm to ensure the antenna did not grow too large. It is expected that a further increase in height would improve performance as it is the equivalent of increasing the ground plane area.

The solution presented was attained through four stages of optimization. Each phase adopted a smaller optimization variable range with an increase in resolution. The optimum chromosome in the final population of each stage seeded the ranges and resolutions of the following stage. The existence of suboptimal solutions was confirmed as the early populations contained substantially different groups of chromosomes with similar fitness (gains within 1 dB of the optimum). Chromosomes situated between these groups exhibited depressed gain, which established the suboptimal solutions.

Fig. 2. Constructed antenna.

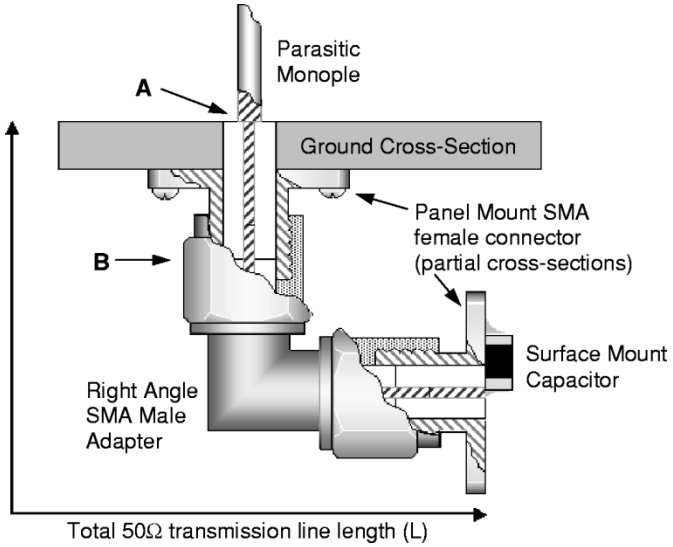

Fig. 3. Example SMA loading.

V. CONSTRUCTION OF THE OPTIMIZED ANTENNA

The antenna structure is simple and thus could be built by hand in a matter of hours. Dual plated PCB formed the antenna ground base while flexible copper sheeting made the skirt. The monopole vias were plated to ensure the radiating elements did not loose energy through the PCBs dielectric. In addition, the plated vias provided ample grounding points within the elemental radius between the top and bottom ground planes. SMA panel mount connectors fed the monopole elements. Fig. 2 presents the constructed antenna.

While varactor diodes would typically be used to produce electrically controlled reactances, their use was inappropriate for simply confirming simulated results. Instead, combinations of SMA adapters terminated with either open circuits, short circuits or surface mount capacitors were used to create the different reactive loads. Fig. 3 shows an example load. At point B, the exact reflection phase length (Γ_ϕ) could be measured with a network analyzer. When added to the ground and panel

connector thickness (AB), the precise reactance at A could be calculated from (5).

This loading configuration however, has a significant section of transmission line. A TL of length L has a Γ_ϕ of

$$\Gamma_\phi = 2\pi\frac{2L}{\lambda} = \frac{4\pi fL}{u} \quad \text{radians.} \tag{7}$$

In (7), λ is the electromagnetic wavelength in the TL at frequency f propagating with velocity u. Thus, its Γ_ϕ change with frequency is

$$\frac{d\Gamma_\phi}{df} = \frac{4\pi L}{u} \quad \text{radians} \cdot Hz^{-1}. \tag{8}$$

Equation (8) shows the change in Γ_ϕ with respect to frequency is not constant when L is variable (as would be the case with different reactances). Therefore, as each reactance changes at a different rate with frequency, the experimental results can only be compared to their simulated counterparts at the reactance design frequency. This however, is sufficient to validate simulation procedure.

The loss of the SMA loading structures was no greater than 0.3 dB. Larger structures incorporating phase shifters had losses in excess of 2 dB and as such, the results they produced had significant error. In addition, the low profile SMA loads had negligible effect on the antenna radiation characteristics.

VI. Antenna Measurement Results

The optimized antenna produced H plane and E plane radiation characteristics that can be seen in Fig. 4. In the azimuth, the antenna's maximum gain reaches 8.08 dBi. Its front-to-back and front-to-null ratios are 10 and 18.8 dB, respectively. This pattern can be reproduced at 60° intervals through the azimuth due to the antenna's symmetry. The main-lobe is elevated at an angle of 4° from the horizontal. Cross-polarization patterns were measured and found to be below 14 dB of the main-lobe gain.

The antenna's mismatch impedance was poor with a measured S_{11} of -7 dB at 2.4 GHz, within 0.4 dB of the computer result. Simulation results of the S_{11} bandwidth showed minimal (within 0.5 dB) degradation over 100 MHz and hence it is clear the S_{11} is not too localized around resonance. This could obviously not be shown experimentally due to (8) but as simulation was so close to experiment, it can safely be assumed correct. If lower levels of S_{11} are required, the problem would have to be reoptimized with weights associated to the directivity and S_{11} in (6).

Fig. 4 shows a clear agreement between the simulated and experimental results. Had the cost function simulated the antenna with inconsistent error, the GA would have converged on a simulated optimum rather than its true counterpart. The similarity between the simulated and experimental results show that the cost function was accurate and hence it is likely the presented solution is the true optimum solution. The simulated gain was degraded by 0.7 dB when compared to experimental testing. However, this error was consistent over a number of different tests and therefore would not have effected the optimization.

When the original antenna (Table I) was optimized with respect to reactance only, an experimental gain no greater than

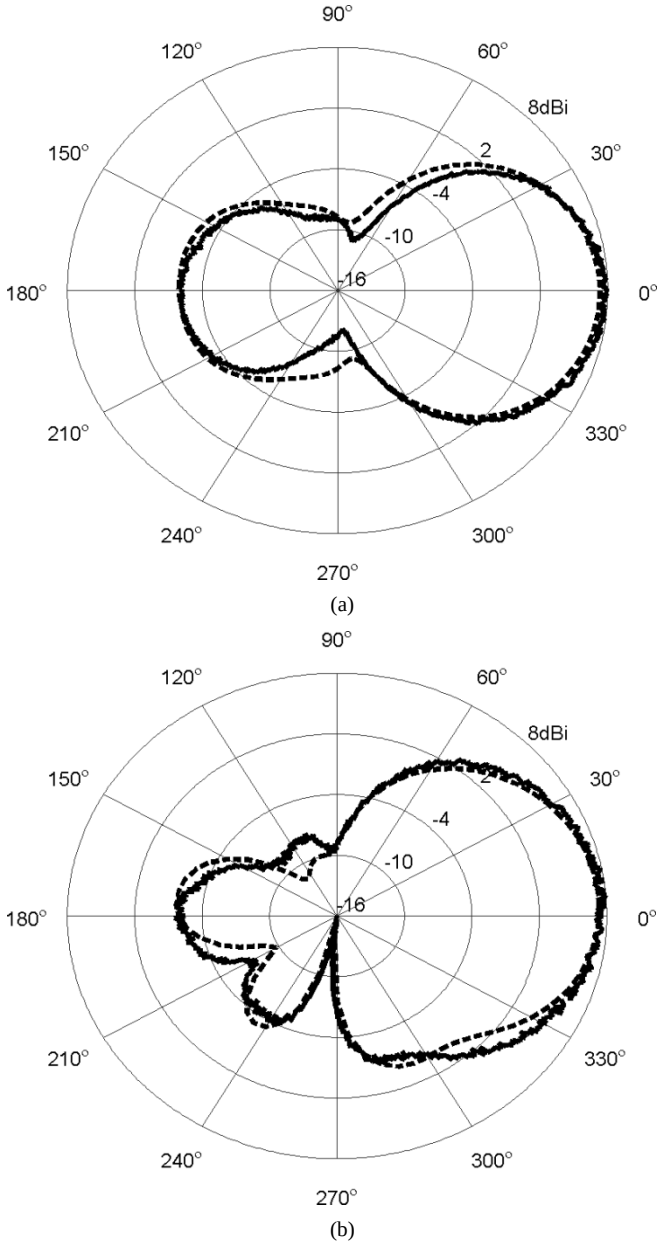

Fig. 4. Radiation characteristics of the optimized ESPAR antenna at 2.4 GHz. (a) H plane radiation $(\theta = 0°)$. (b) E plane radiation $(\phi = 0°)$;—Experimental—HFSS.

6.7 dBi was achieved. In addition, the main lobe was elevated at 25°. Conversely, regardless of the finite ground plane, the optimized antenna has minimal lobe elevation and a gain of 8.08 dBi. This reduction in main-lobe elevation is one of the principal reasons for the increase in azimuth gain. To reject the possiblilty that the reactance-structure combination fluked a suppression of main-lobe elevation, a further 10 random, nonoptimized reactance loading cases were tested. Main-lobe elevations were recorded between 0° and 15° with a mean of 9.7°. Horizontal gains were no less than 0.5 dB of the elevated gains. This is in contrast to the original antenna's average elevation of 25° with horizontal gains between 1 and 1.6 dB less than the elevated gains. These results suggest the optimized structure of the antenna has reduced the main lobe elevation independent of the reactance loading.

While the structural optimization has netted an increase in gain of approximately 1.4 dB over the reactive optimization, this could potentially translate to 2.8 dB in a system environment, which is equivalent to a significant reduction in transmitter power of approximately 48%. In addition, showing that an accurate structural simulation works, has laid foundations for immersing the antenna in dielectric to reduce it to a more practical size as has been proposed previously [23].

VII. Conclusion

A horizontal gain optimized electrically steerable passive array radiator antenna designed for use in an *ad hoc* wireless network has been presented. The antenna was optimized with respect to gain to reduce interference and transmission powers in a system. In a homogeneous *ad hoc* network, any optimization in the gain of an antenna will potentially have double the effect in the system.

The optimization solution space of the ESPAR antenna was very large, and polluted by localized, suboptimal solutions. Accordingly, a genetic algorithm was used for optimization because of its robust nature. The GA employed a FEM based cost function in order to obtain accurate modeling of the antenna. Both physical antenna structure and loading reactances were optimized.

As a result, a circular monopole array of radius 0.308λ surrounding a single feed monopole based on a 0.48λ radius ground plane bounded with a 0.276λ skirt was designed. All monopole heights were 0.216λ at 2.4 GHz. The antenna produced a maximum gain of 8.08 dBi with average main-lobe elevation angles of 9.7°. With increases in computing power, the optimization process used could readily be adapted to more complex optimization problems like that of the antenna immersed in a dielectric medium to reduce physical size.

References

[1] S. L. Preston, D. V. Thiel, and J. W. Lu, "A multibeam antenna using switched parasitic and switched active elements for space-division multiple access applications," *IEICE Trans. Commun.*, vol. E82-C, pp. 1202–1210, July 1999.

[2] S. L. Preston, D. V. Thiel, T. A. Smith, S. G. O'Keefe, and J. W. Lu, "Base-station tracking in mobile communications using a switched parasitic antenna array," *IEEE Trans. Antennas Propagat.*, vol. 46, pp. 841–844, June 1998.

[3] D. V. Thiel and S. L. Smith, *Switched Parasitic Antennas for Cellular Communications*. Norwood, MA: Artech House, 2002.

[4] T. Ohira and K. Gyoda, "Electronically steerable passive array radiator antennas for low-cost analog adaptive beamforming," in *Proc. IEEE Int. Conf. Phased Array Syst. Technol.*, 2000, pp. 101–104.

[5] T. Ohira, "Adaptive array antenna beamforming architectures as viewed by a microwave circuit designer," in *Proc. Asia-Pacific Microwave Conf.*, Sydney, 2000, pp. 828–833.

[6] T. Ohira and K. Gyoda, "Handheld microwave direction-of-arrival finder based on varactor-tuned aerial beamforming," in *Proc. Asia-Pacific Microwave Conference*, Taipei, Taiwan, 2001, pp. 585–588.

[7] D. Goldberg, *Genetic Algorithms in Search, Optimization, and Machine Learning*. Reading, MA: Addison-Wesley, 1989.

[8] K. Gyoda, Y. Kado, Y. Ohno, K. Hasuike, and T. Ohira, "WACNet: wireless *ad hoc* community network," in *Proc. IEEE Int. Symp. Circuits Systems ISCAS2001, IV*, Sydney, 2001, pp. 862–865.

[9] D. V. Thiel, "Tin-can antenna—a switched parasitic monopole antenna on a finite ground plane with a conductive sleeve," in *Proc. CSIRO 7th Australian Symp. Antennas*, 2001, p. 19.

[10] Y. Ojiro, H. Kawakami, K. Gyoda, and T. Ohira, "Improvement of elevation directivity for ESPAR antennas with finite ground plane," in *Proc. IEEE 2001 Antennas Propagat. Soc. Symp.*, Boston, MA, 2001, pp. 18–19.

[11] HFSS v8.0 (2002, Feb.). *http://www.ansoft.com* [Online]

[12] J. Cheng, Y. Kamiya, and T. Ohira, "Adaptive beamforming of ESPAR antenna based on steepest gradient algorithm," *IEICE Trans. Commun.*, vol. E84-B, pp. 1790–1800, July 2001.

[13] B. Shishkov, J. Cheng, and T. Ohira, "Adaptive control algorithm of ESPAR antenna based on stochastic approximation theory," *IEICE Trans. Commun.*, vol. E85-B, no. 4, pp. 802–811, Apr. 2002.

[14] R. Schlub, W. Lu, and T. Ohira, "Frequency characteristics of the ESPAR antenna," in *Proc. Asia Pacific Microwave Conf.*, Taipei, Taiwan, 2001, pp. 697–700.

[15] Q. Han, K. Inagaki, K. Iigusa, R. Schlub, T. Ohira, and M. Akaike, "Harmonic distortion suppression technique for varactor-loaded parasitic radiator antennas," *IEICE Trans. Commun.*, vol. E85-C, pp. 2015–2021, Dec. 2002.

[16] C. A. Balanis, *Antenna Theory Analysis and Design*. New York: Harper & Row, 1982.

[17] D. M. Pozar, *Microwave Engineering*, 2nd ed. New York: Wiley, 1998.

[18] E. E. Altshuler and D. S. Linden, "Design of a loaded monopole having hemispherical coverage using a genetic algorithm," *IEEE Trans. Antennas Propagat.*, vol. 45, pp. 1–4, Jan. 1997.

[19] Z. Altman, R. Mittra, and A. Boag, "New designs of ultra wide-band communication antennas using a genetic algorithm," *IEEE Trans. Antennas Propagat.*, vol. 45, pp. 1494–1505, Oct. 1997.

[20] R. Schlub, D. V. Thiel, J. W. Lu, and S. G. O'Keefe, "Dual-band six-element switched parasitic array for smart antenna cellular communications systems," *Electron. Lett.*, vol. 36, pp. 1342–1343, Aug. 2000.

[21] D. S. Weile and E. Michielssen, "Genetic algorithm optimization applied to electromagnetics: a review," *IEEE Trans. Antennas Propagat.*, vol. 45, pp. 343–353, Mar. 1997.

[22] V. R. Vemuri and W. Cedeno, "Multi-niche crowding for multi-nodal search," in *Practical Handbook of Genetic Algorithms—New Frontiers*, L. Chambers, Ed. Boca Raton, FL: CRC, 1995, vol. 2, pp. 6–10.

[23] J. Lu, D. Thiel, B. Hanna, and S. Saario, "Dielectric embedded electronically switched and multiple beam antenna arrays for wireless communication systems," *Electron. Lett.*, vol. 37, pp. 871–872, July 2001.

Robert Schlub received the B.E. degree in microelectronic engineering from Griffith University, Queensland, Australia, in 2000, where he is currently working toward the Ph.D. degree.

In 2001, he held a one-year internship with the ATR Adaptive Communications Research Laboratories, Kyoto, Japan.

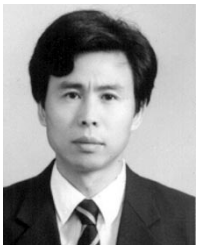

Junwei Lu (M'92) received the B.E. degree from the Department of Electrical Engineering, Xian Jiaotong University, China, in 1976, the M.E. degree in electronic and computer engineering from the National Toyama University, Japan, in 1988, and the Ph.D. degree in electrical and computer engineering from the National Kanazawa University, Japan, in 1991.

From 1976 to 1984, he was with the Institute of Qinhai Electric Power Testing and Research, China, where he was involved in various national research projects for the electrical power industry. Since 1985, he has resumed academic study and research in the area of computational electromagnetics with the Laboratory of Electrical Communications, Toyama University. Since 1988, he worked on applied computational electromagnetics and was involved in the development of magnetic devices with the Laboratory of Electrical Energy Conversion, Kanazawa University. He joined the School of Microelectronic Engineering at Griffith University in 1992, where he is now an Associate Professor. His fields of interest include computational and visual electromagnetics, high-performance cluster computing, smart mobile terminal antennas, RF/MW devices and circuits, and high-frequency magnetics.

Takashi Ohira (S'79–M'83–SM'99) was born in Osaka, Japan, in April 1955. He received the B.E. and D.E. degrees in communication engineering from Osaka University, Osaka, in 1978 and 1983, respectively.

In 1983, he joined NTT Electrical Communication Laboratories, Yokosuka, Japan, where he was engaged in research on monolithic integration of microwave semiconductor devices and circuits. He developed GaAs MMIC transponder modules and microwave beam-forming networks aboard Japanese domestic multibeam communication satellites, Engineering Test Satellite VI (ETS-VI) and ETS-VIII, at NTT Wireless Systems Laboratories, Yokosuka. Since 1999, he has been engaged in research on wireless *ad hoc* networks and microwave analog adaptive antennas aboard consumer electronic devices at ATR Adaptive Communications Research Laboratories, Kyoto, Japan. Concurrently, he was a Consulting Engineer for National Astronautical Space Development Agency (NASDA) ETS-VIII Project in 1999, and an Invited Lecturer for Osaka University in 2000 to 2001. He coauthored *Monolithic Microwave Integrated Circuits* (Tokyo: IEICE, 1997).

Dr. Ohira serves as IEEE MTT-S Japan Chapter Vice-Chairperson. He was awarded the 1986 IEICE Shinohara Prize and 1998 Japan Microwave Prize.